Synthesis of ferrite and nickel ferrite nanoparticles using radio-frequency thermal plasma torch

S. Son and M. Taheri
Department of Materials Science and Engineering, Carnegie Mellon University, Pittsburgh, Pennsylvania 15213

E. Carpenter and V. G. Harris
U.S. Naval Research Laboratory, Washington, D.C. 20375-5000

M. E. McHenry
Department of Materials Science and Engineering, Carnegie Mellon University, Pittsburgh, Pennsylvania 15213

Nanocrystalline (NC) ferrite powders have been synthesized using a 50 kW–3 MHz rf thermal plasma torch for high-frequency soft magnet applications. A mixed powder of Ni and Fe (Ni:Fe = 1:2), a NiFe permalloy powder with additional Fe powder (Ni:Fe=1:2), and a NiFe permalloy powder (Ni:Fe=1:1) were used as precursors for synthesis. Airflow into the reactor chamber was the source of oxygen for oxide formation. XRD patterns clearly show that the precursor powders were transformed into NC ferrite particles with an average particle size of 20–30 nm. SEM and TEM studies indicated that NC ferrite particles had well-defined polygonal growth forms with some exhibiting (111) faceting and many with truncated octahedral and truncated cubic shapes. The Ni content in the ferrite particles was observed to increase in going from mixed Ni and Fe to mixed permalloy and iron and finally to only permalloy starting precursor. The plasma-torch synthesized ferrite materials using exclusively the NiFe permalloy precursor had 40%–48% Ni content in the Ni-ferrite particle, differing from the $NiFe_2O_4$ ideal stoichiometry. EXAFS was used to probe the cation coordination in low Ni magnetite species. The coercivity and Neel temperature of the high Ni content ferrite sample were 58 Oe and ~590 °C, respectively. © *2002 American Institute of Physics.* [DOI: 10.1063/1.1452705]

Due to their large resistivities, ferrites are of great importance as high-frequency magnetic materials. Spinel-type oxides (MFe_2O_4 where M is a divalent metal), which include the magnetic ferrites, are often denoted by the formula AB_2O_4 where A and B refer to tetrahedral and octahedral sites, respectively, in the fcc oxygen lattice. The equilibrium distribution of cations in the spinel structure depends on ionic radii, electronic configuration, electrostatic energies, and polarization effects. Nonequilibrium cation distributions are possible using novel or nonequilibrium processing routes. A nonequilibrium distribution of cations in the spinel structure can influence the intrinsic magnetic properties of these materials.[1]

Considering losses, the materials of choice for many microwave applications, are cubic ferrites. Of the cubic spinel ferrites, two classes of materials are significant; the Mn–Zn and the Ni–Zn(Cu) ferrite materials. Mn–Zn ferrite is typically limited to frequencies <500 kHz owing to their relatively low resistivities (0.02–20_-m); Ni–Zn ferrite materials have very large resistivities (10^1–10^7_-m), high Neel temperatures above 500 °C and tunable magnetic inductions making them potential candidates for much higher-frequency (1–300 MHz) applications.[2]

NC ferrites with particle sizes well below the microwave skin depth may offer promise as low loss materials at high frequencies. It is our goal to synthesize NC magnetite (Fe_3O_4) and nickel ferrites ($NiFe_2O_4$) from metallic precursors by radio frequency (rf) plasma torch synthesis and study their growth forms, cation distributions, and magnetic properties.

A rf plasma system consisting of a TEKNA PL50 type plasma torch head with a 50 kW, 3 MHz power supply and a gas expansion reactor chamber connected to a filtering unit was used for producing the NC powder. Argon was used as plasma gas and the sheath gas consisted of a mixture of Ar and H_2. Precursor powder was injected through the plasma stream using Ar, as a carrier gas. After the plasma ignited, air was introduced into the reaction chamber as a source of oxygen. Then the final powders from both the reaction chamber and the dry filter were collected and analyzed. More detailed processing procedures are described elsewhere.[3–5]

Three types of precursor samples were prepared for the plasma torch. Precursor sample 1 was a mixture of pure Ni (<149 μm, Aldrich Chemical Co.) and pure Fe powder (6–10 μm, Alfa Aesar Co.) at the atomic ratio of 1:2 (i.e., that of the desired cation ratio). After low energy ball milling, it had an average grain size of 20 μm with a disk-shape morphology. Sample 2 was a mixture of NiFe (1:1) permalloy powder (<38 μm, supplied by the Magnetics Division of Spang, Butler, PA) and pure Fe powder with overall Ni:Fe ratio=1:2. Sample 3 was a permalloy NiFe powder (Ni:Fe =1:1, <38 μm).

X-ray diffraction (XRD) characterization of both the precursor powders and the as-synthesized powders was carried out on a Rikagu diffractometer using Cu $K\alpha$ radiation. Scanning electron microscopy (SEM) using a Philips XI-30 FEG
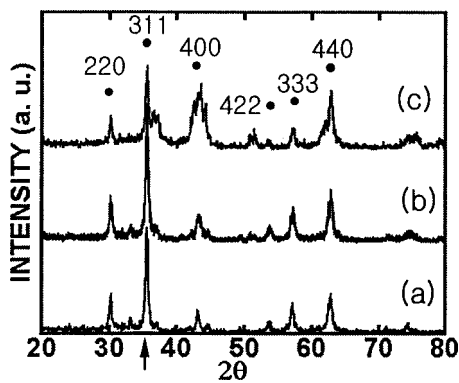
7589

FIG. 1. X-ray diffraction patterns; _-NiFe$_2$O$_4$ peaks, ↑-2θ_B=35.742°; (a) Ni+Fe plasma-torched powder (average grain size=20 nm), (b) NiFe+Fe plasma-torched powder (26 nm), (c) NiFe plasma-torched powder (18 nm).

TABLE I. Ni content in powder before and after plasma torch (PT) process measured by EDX in TEM.

Sample no.	Before PT		After PT	
	Ni content (%)	H_C (Oe)	Ni content (%)	H_C (Oe)
1	33.3	60	~4	110
2	33.3	30	~15	60
3	50	37	40~48	58

model and high-resolution transmission electron microscopy (HRTEM) on a TECNAI F20 model with energy dispersion x-ray (EDX) were used to examine the morphology and composition of particles. The chemistry of the ferrites was further studied by Inductive Coupled Plasma (ICP) chemical analysis (Perkin-Elmer Optima 2000 DV ICP-OES), EXAFS, and EDX analysis.

Extended x-ray absorption fine structure (EXAFS) spectra for the first ferrite sample (nominally magnetite) were collected at the Brookhaven National Laboratory beam line (X23B). Spectra encompassing the Fe (7112 eV) K absorption edge over an energy range that extended from 100 eV to 800 eV beyond the edge energy were employed.[6] Data were analyzed following standard EXAFS procedures leading to the Fourier transformation of data to radial coordinates. In this form, the transform profile reflects the average local environment around absorbing atoms.[7] The peak amplitudes reflect the occupancy of atomic shells and their dynamic and static disorder. The radial coordinate of the peaks reflects the distance of atomic shells from the absorber that are uncorrected for an electron phase shift intrinsic to EXAFS. This phase shift must be calculated separately and added to the data to determine actual bond distances.

The magnetic properties of the samples were obtained with a high temperature vibrating sample magnetometer (VSM; Lake Shore Model 7300, with 1000 °C oven assembly) and a superconducting quantum interference device (SQUID; Quantum Design PPMS).

XRD on as-synthesized powders revealed that most of the precursor powders were transformed to NC ferrites (Fig. 1). All major peaks can be indexed to the standard pattern for ferrite, Fe$_3$O$_4$ (or nickel ferrite NiFe$_2$O$_4$) (JCPDS No. 03-875). Some tiny peaks observed may correspond to small amounts of unreacted precursor powders. The symmetry and lattice spacings of ferrite, Fe$_3$O$_4$, and nickel ferrite NiFe$_2$O$_4$ are nearly identical making it nearly impossible to distinguish them on the basis of XRD, especially with the large peak broadening characteristic of the NC size.

The average particle size was estimated from the so-called Scherrer formula.[8] The ferrite (311) peak corresponding to 2θ_B=35.743° (JCPDS No. 03-875) was employed for calculating an average particle size. The Scherrer analysis

indicates (confirmed by TEM pictures) that the average grain size of all the samples were reduced from the 20–30 μm starting powder size to 20–30 nm after plasma synthesis.

ICP analysis, EDX, and EXAFS on sample 1 indicated that the mixed Fe and Ni powders did not result in alloying of Fe and Ni, nor did alloying occur in the plasma. Powders collected from the plasma torch filter were primarily magnetite (with 3–4 at. % Ni). These powders then consisted of magnetite with small amounts of Ni incorporated and were NC. The concentration of Ni content in ferrite particles of each sample was shown in Table I. Sample 1 and sample 2 were determined to have Ni concentrations of ~4% and ~15%, respectively, both differing significantly from that of stoichiometric NiFe$_2$O$_4$. Sample 3, a plasma-torched synthesized using only a (50:50 Ni–Fe) permalloy powder precursor, had a Ni content of 40%–48% in the particles nearly consistent with a stoichiometric Ni ferrite. To our knowledge this represents the first successful rf plasma torch synthesis of Ni ferrites. Our results demonstrate the viability of plasma torch synthesis for production of ferrite particles. However, more research will be required for optimum control of the Ni stoichiometry of the particles.

EXAFS analysis was performed on the initially produced magnetite powders. Figure 2 shows the Fourier transformed Fe EXAFS data, uncorrected for the electron phase shift. The nearest neighbor metal (Fe)–oxygen bond appears at r~1.4 Å, corresponding to the tetrahedrally coordinated absorbing cation, whereas the oxygen bond near 1.9 Å corresponds to the octahedrally coordinated cation. The large peak centered near r=2.6 Å corresponds with the cation–
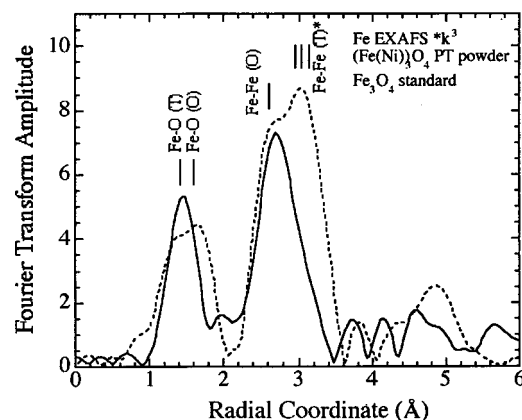

FIG. 2. Fourier transformed Fe EXAFS data, uncorrected for the electron phase shift for ferrite powder processed using the plasma torch (denoted PT in Fig. 2) to that of Fe$_3$O$_4$ data corresponding to a sample prepared by ceramic means.
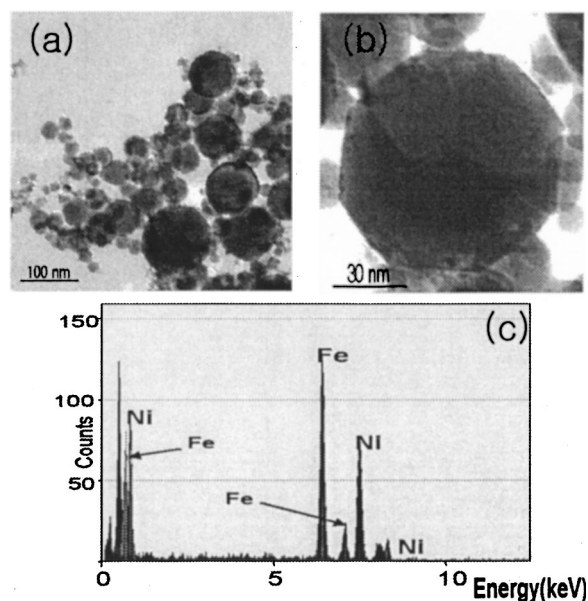
FIG. 3. TEM images: (a) sample 3 plasma-synthesized powder showing particle size distribution, (b) examples of truncated octahedral faceted powders, (c) EDX spectrum of the same.

FIG. 4. Magnetization vs temperature curve: (a) sample 1 ($T_N= \sim 590\,°C$), (b) sample 3 ($T_N = \sim 590\,°C$).

Magnetic hysteresis curves were measured using VSM at room temperature. Coercivities values, H_C, are summarized in Table I. Figure 4 shows magnetization as a function of temperature for samples 1 and 3 as measured with high temperature VSM. The Neel temperature (T_N) of sample 1 is $\sim 590\,°C$ and its mass saturation magnetization (M_S measured in SQUID) value at room temperature (RT) is 55.56 emu/g. Sample 3 has a T_N of $\sim 590\,°C$ and an RT M_S of 35.53 emu/g. Ni is observed to reduce the magnetic moment of the ferrite as is observed in bulk ferrites. The Neel temperatures of bulk magnetite and Nickel ferrite are nearly identical and near 590 °C.

cation distance when both the absorbing cation and scattering cation reside on the octahedral sublattice. This is a unique fingerprint identifying the absorbing ion as residing on the octahedral sites and allows for the determination of octahedral sublattice occupation. The peak centered near 3.1 Å occurs for an absorber on the tetrahedral sublattice, but the identification is not unique.[9] In comparing the ferrite powder processed using the plasma torch (denoted PT in Fig. 2) to that of the Fe_3O_4 data corresponding to a sample prepared by ceramic means, one sees that the Fourier amplitude corresponding to tetrahedral coordination is substantially reduced. This reduction of amplitude is commonly seen in comparing nanoparticles to larger particles where surface truncation of the lattice reduces the average coordination of the absorbing species. Further, it has recently been reported by Harris *et al.*[10] that nanoparticles are more prone to vacancy stabilization in the bulk spinels. These authors postulate that a surface strain mechanism is responsible.

TEM analysis on ferrite powder revealed the results that NC ferrite particles had well-defined polygonal growth forms some exhibiting (111) faceting and many with octahedral or truncated octahedral shapes (Fig. 3). In order to understand the polygonal faceting in the synthesized powders, a more exhaustive analysis of the TEM observed morphologies with computer simulation of the growth forms will be performed. It is interesting to note that hexoctahedral growth forms have been observed in magnetite nanocrystals found in Martian meteorites. These truncated hexoctahedral forms are uncommon for magnetite observed on earth, with the exception of magnetite particles observed in magnetotactic bacteria.[11,12]
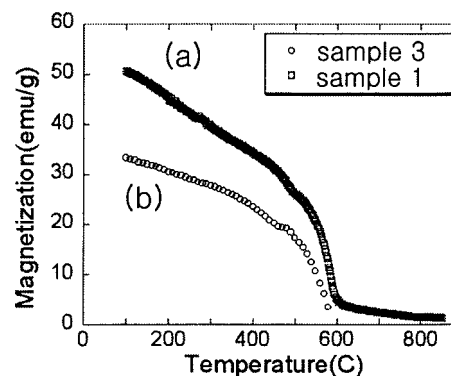
[1] T. Seshagiri Rao, *Ferrite Materials—Science & Technology*, edited by B. Viswanathan and V. R. K. Murthy (Narosa, 1990), Chap. 1, pp. 2–17, Chap. 3, pp. 39–53.
[2] E. C. Snelling, *Soft Ferrites: Properties and Applications* (Butterworths, London, 1988).
[3] Z. Turgut, CMU Ph.D. thesis.
[4] J. H. J. Scott *et al.*, in Surface-Controlled Nanoscale Materials for High-Added-Value Applications, MRS Sym. Proc. Vol. 501, edited by K. E. Gonsalves *et al.*, pp. 121–126 (1998).
[5] M. I. Boulos, High. Temp. Chem. Processes **1**, 401 (1992).
[6] Data collection was performed in transmission mode at the Naval Research Laboratory's Materials Analysis beamline (X23B) at the National Synchrotron Light Source (Brookhaven National Laboratory, Upton, NY). For optical design and performance see: R. A. Neiser *et al.*, Nucl. Instrum. Methods Phys. Res. A **266**, 220 (1988). At the time data were collected the storage ring energy was 2.54 GeV and the ring current ranged from 180–250 mA.
[7] D. E. Sayers and B. Bunker, in *X-ray Absorption: Basic Principles of EXAFS, SEXAFS, and XANES*, edited by D. C. Konigsberger and R. Prins (Wiley, New York, 1988).
[8] B. D. Cullity, *Elements of X-ray Diffraction*, 2nd ed. (Addison-Wesley, New York, 1978), pp. 101–102.
[9] V. G. Harris, *et al.*, IEEE Trans. Magn. **31**, 3473 (1995).
[10] V. G. Harris, *et al.*, J. Magn. Soc. Jpn. **22**, 157 (1998).
[11] K. L. Thomas-Keprta, *et al.*, PNAS **98**, 2164 (2001).
[12] D. C. Golden, *et al.*, Am. Mineral. **86**, 370 (2001).